A ferrimagnetic bilayer system in an applied transverse field

1993 J. Phys.: Condens. Matter 5 6313

(http://iopscience.iop.org/0953-8984/5/34/017)

J. Phys.: Condens. Matter 5 (1993) 6313–6322. Printed in the UK

A ferrimagnetic bilayer system in an applied transverse field

M Jaščur† and T Kaneyoshi
Department of Physics, Nagoya University, 464-01 Nagoya, Japan

Received 2 February 1993, in final form 8 March 1993

Abstract. The magnetic properties of a ferrimagnetic bilayer system consisting of spin-$\frac{1}{2}$ and spin-$\frac{3}{2}$ Ising layers in an applied transverse field are examined by the use of effective-field theory. We have obtained some interesting results that may potentially be related to experimental work on rare-earth/transition-metal multilayer films.

1. Introduction

Recently, multilayers composed of rare-earth (RE) and transition-metal (TM) single layers have been grown on some substrates [1–5]. These materials are now of great interest because they are new materials with interesting and possibly useful properties for technological applications as well as academic research. However, most of the theoretical work related to magnetic multilayered systems has been restricted to Ising or Heisenberg systems consisting of only spin-$\frac{1}{2}$ ions where each layer has a coupling constant of a different magnitude [6–11]. Therefore, in order to treat RE/TM multilayers, it is necessary to discuss magnetic multilayers with different spins.

The RE/TM multilayers show an interesting magnetic coupling behaviour. The 3d–4f indirect interaction is considered to be negative for heavy REs, while it is positive for light REs. Owing to the interaction, multilayer films of RE (Tb, Gd)/TM (Co, Fe) show a ferrimagnetic behaviour, for the small thicknesses of these materials [3, 5]. Furthermore, the compensation temperature depends strongly on the thickness.

Very recently, the magnetic properties of bilayer systems consisting of two ferromagnetic Ising layers A ($S_A = \frac{1}{2}$) and B ($S_B = \frac{3}{2}$) coupled ferrimagnetically have been examined by the use of the effective-field theory [12, 13], in order to explain the experimental data for RE/TM multilayer films with equal thicknesses [3, 5]. In the process, a number of interesting phenomena has been found. On the other hand, the theoretical framework [13] has also been extended to the transverse Ising model with an arbitrary spin S [14, 15].

In this work, we shall study via the same method as in [13–15] the effects of the applied transverse field (i.e., the field is applied parallel to the bilayer plane) on the magnetic properties of a ferrimagnetic bilayer Ising system consisting of spin-$\frac{1}{2}$ ($S_A = \frac{1}{2}$) and spin-$\frac{3}{2}$ ($S_B = \frac{3}{2}$) ferromagnetic monolayers. In contrast to previous work [6], however, the single-ion anisotropy on layer B is not taken into account in this work. The results obtained here may be useful for future experimental work. In particular, a magnetic field applied parallel to the bilayer plane (or RE/TM multilayer film plane) may control the compensation point, which is observed in the easy z direction perpendicular to the bilayer plane.

† Permanent address: Department of Theoretical Physics and Geophysics, Faculty of Natural Sciences, P J Šafarik University, Moyzesova 16, 041 54 Košice, Slovakia.

0953-8984/93/346313+10$07.50

The outline of this paper is as follows. In section 2, the basic relations for obtaining phase diagrams and magnetizations in the x and z directions are given briefly. The numerical results are shown and discussed in section 3. In section 4, the internal energy and specific heat are obtained and discussed.

2. Formulation

We consider the bilayer system with a negative interlayer coupling J_3 in an applied transverse field Ω. For simplicity, we restrict our attention to the case of a simple cubic Ising-type structure without any single-ion anisotropy on the B monolayer. The two-dimensional cross section of the system is depicted in figure 1. The Hamiltonian of the system is given by

$$\mathcal{H} = -J_1 \sum_{i,j} \mu_i^z \mu_j^z - J_2 \sum_{m,n} S_m^z S_n^z - J_3 \sum_{i,m} \mu_i^z S_m^z - \Omega \left(\sum_m S_m^x + \sum_i \mu_i^x \right) \tag{1}$$

where the first three sums are taken over all the nearest-neighbour pairs only once, μ_i^x, μ_i^z are the components of spin-$\frac{1}{2}$ operators on A layers and the S_i^x, S_i^z are the components of spin-$\frac{3}{2}$ operators on B layers. There exist three coupling constants depending on where the spin pair is located. In order to relate our system to some experimental data for RE/TM multilayer systems, we take $J_1 > J_2 > 0$. That is to say, A layers consist of TM atoms and B layers are made up of RE atoms. Then, the exchange interaction J_1 between A atom pairs results from the direct interaction and the interaction J_2 between B atom pairs is considered to be due to the indirect interaction. Furthermore, the J_3 (or 3d–4f indirect interaction) is taken to be negative.

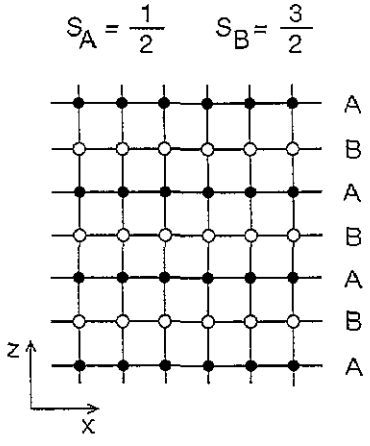

Figure 1. Part of the two-dimensional cross section through the magnetic bilayer system consisting of the two ferromagnetic ($J_1 \geqslant 0$, $J_2 \geqslant 0$) monolayers A and B with spins $S_A = \frac{1}{2}$ and $S_B = \frac{3}{2}$.

In this section, we shall briefly review the basic framework of [12–15], since the basic spin identities for homogenous systems with an arbitrary spin in a transverse field have been derived in [14] and [15] and the basic thermodynamical quantities of the bilayer system in figure 1 have been formulated within the effective-field theory (EFT) in [12]. In particular, [15] reviews how the spin-S transverse Ising model as well as the spin-S ($S \geqslant \frac{1}{2}$) Ising model can be formulated on the basis of the Ising spin identities and the differential operator

technique. From this work, we can straightforwardly obtain relations for the longitudinal and transverse magnetization in the A and B layers as follows:

$$\sigma_z = \langle \mu_i^z \rangle = [\cosh(\tfrac{1}{2} J_1 \nabla) + 2\sigma_z \sinh(\tfrac{1}{2} J_1 \nabla)]^4 \times [\cosh(\eta J_3 \nabla) + (m_z/\eta) \sinh(\eta J_3 \nabla)]^2 F_A(x)|_{x=0} \tag{2}$$

$$m_z = \langle S_i^z \rangle = [\cosh(\eta J_2 \nabla) + (m_z/\eta) \sinh(\eta J_2 \nabla)]^4 \times [\cosh(\tfrac{1}{2} J_3 \nabla) + 2\sigma_z \sinh(\tfrac{1}{2} J_3 \nabla)]^2 F_B(x)|_{x=0} \tag{3}$$

$$\sigma_x = \langle \mu_i^x \rangle = [\cosh(\tfrac{1}{2} J_1 \nabla) + 2\sigma_z \sinh(\tfrac{1}{2} J_1 \nabla)]^4 \times [\cosh(\eta J_3 \nabla) + (m_z/\eta) \sinh(\eta J_3 \nabla)]^2 H_A(x)|_{x=0} \tag{4}$$

$$m_x = \langle S_i^x \rangle = [\cosh(\eta J_2 \nabla) + (m_z/\eta) \sinh(\eta J_2 \nabla)]^4 \times [\cosh(\tfrac{1}{2} J_3 \nabla) + 2\sigma_z \sinh(\tfrac{1}{2} J_3 \nabla)]^2 H_B(x)|_{x=0}. \tag{5}$$

Furthermore, it is necessary to evaluate the parameter $q_z \equiv \eta^2$ which is given by

$$q_z = \langle (S_i^z)^2 \rangle = [\cosh(\eta J_2 \nabla) + (m_z/\eta) \sinh(\eta J_2 \nabla)]^4 \times [\cosh(\tfrac{1}{2} J_3 \nabla) + 2\sigma_z \sinh(\tfrac{1}{2} J_3 \nabla)]^2 G_B(x)|_{x=0}. \tag{6}$$

In the above equations, $\nabla = \partial/\partial x$ is a differential operator, N denotes the total number of atoms in the A (or B) layer and the functions $F_\alpha(x)$, $G_\alpha(x)$ and $H_\alpha(x)$ ($\alpha = A, B$) are defined in the appendix.

In order to obtain (2)–(6), we have used the relation

$$\exp(a S_m^z) = \cosh(\eta a) + (S_m^z/\eta) \sinh(\eta a) \tag{7}$$

which can be viewed as an approximated Van der Waerden identity valid for an arbitrary spin. Moreover, the multisite correlations appearing in the process of calculation have been decoupled as follows:

$$\langle \mu_j^z S_k^z \ldots \mu_l^z \rangle \cong \langle \mu_j^z \rangle \langle S_k^z \rangle \ldots \langle \mu_l^z \rangle \tag{8}$$

for $j \neq k \neq \ldots \neq l$. The main reason for the introduction of both approximations is to avoid mathematical complexities that naturally appear if we treat any physical problem with spin higher than one beyond the standard mean-field approximation. In particular, the application of relation (7) brings a substantial reduction of algebraic calculations. In fact, if one does not use (7), they become mathematically tractable but rather complicated problems. In our previous work [12–15], we have found that treatments based on the approximations (7) and (8) provide reasonable results that are better than the mean-field results. This is due to the fact that relations (7) and (8) allow us to account for some correlations through the parameter q_z (or η), which gives a very important contribution to the temperature or field dependences of thermodynamical quantities. Therefore, the results predicted by EFT cannot be obtained within the mean-field theory where all the correlations are completely ignored.

Here, we define the total magnetizations M_α in the α direction ($\alpha = x, z$) as

$$M_\alpha = \tfrac{1}{2}(\sigma_\alpha + m_\alpha). \tag{9}$$

After expanding the right-hand sides of (2)–(5), one obtains a close set of polynomial equations with coefficients depending on T, Ω, J_1, J_2 and J_3 that can be solved numerically. In the next section, we shall show some typical results obtained through the numerical analysis of the above-mentioned equations.

3. Numerical results

3.1. Phase diagram

Let us first study the dependences of the transition temperature T_c and the compensation temperature T_{comp} on the transverse field Ω and exchange interaction parameters J_2 and J_3. The transition temperature can be obtained by expanding the right-hand side of (2) and (3) and keeping only the terms linear in σ_z and m_z; in a finite transverse field, the μ_i^z and S_m^z components of the system are disordered at high temperatures, but below a transition temperature T_c they order and take $\sigma_z \neq 0$ and $m_z \neq 0$, although there is an order with $\sigma_x \neq 0$ and $m_x \neq 0$ at all temperatures. Thus, the coupled equations for evaluating T_c are given in the matrix form

$$\mathbf{M}\begin{pmatrix}\sigma_z\\ m_z\end{pmatrix} = \begin{pmatrix}A_1 - 1 & A_2\\ B_1 & B_2 - 1\end{pmatrix}\begin{pmatrix}\sigma_z\\ m_z\end{pmatrix} = 0 \tag{10}$$

where the coefficients A_n and B_n ($n = 1, 2$) can be obtained from (2) and (3). The transition temperature can be determined from $\det \mathbf{M} = 0$. Then, the parameter η is included in the coefficients, and it can be determined by solving

$$\eta^2 = \cosh^4(\eta J_2 \nabla)\cosh^2(\tfrac{1}{2}J_3\nabla)G_B(x)|_{x=0} \tag{11}$$

at $T = T_c$. On the other hand, the compensation temperature T_{comp} of the system can be evaluated by requiring the condition $M_z = 0$ in the coupled equations (2) and (3).

Some typical results for the phase diagram of the bilayer system are depicted in figure 2 by selecting $J_2/J_1 = 0.05$. In the figure, the full and broken curves represent the variations of T_{comp} and T_c, respectively.

Figure 2(a) shows the phase diagram in the (T_c, $|J_3|/J_1$) space when a positive value of Ω is selected. Here, the results for $\Omega = 0.0$ are equivalent to those of $D/J_1 = 0.0$ labelled c in figure 2 of [12]. The results of figure 2(a) clearly express how the T_{comp} and T_c can be changed with the increase of the applied transverse field. In particular, it gradually becomes impossible to find the compensation point when the value of Ω increases. The situation is depicted in the figure as a chain curve; for a large Ω, one cannot find the T_{comp} of the system for very small values of $|J_3|/J_1$.

At this point, we known from the study of the transverse Ising model that with the increase of Ω the transition temperature T_c falls from its value at $\Omega = 0.0$ and reaches zero at a critical value Ω_c. For the bilayer system with $J_2/J_1 = 0.05$, the phenomenon is plotted in figure 2(b) by taking three values of J_3/J_1, namely $J_3/J_1 = -0.2$, -0.5 and -1.0. In figure 3, therefore, the critical value Ω_c at which T_c of the bilayer system reduces to zero is depicted as a function of $|J_3|/J_1$ by selecting three values of J_2/J_1.

Now, an interesting phenomenon is also obtained in figure 2(b): T_{comp} may change with the value of Ω. For example, the T_{comp} of the bilayer system with $J_3/J_1 = -0.2$ can be found even at $\Omega = 0.0$. Increasing the value of Ω, it falls from its value at $\Omega = 0.0$ and reaches zero, like the T_c curves. For the bilayer system with a certain value of J_3/J_1 smaller than $J_3/J_1 = -0.2$, on the other hand, T_{comp} cannot be obtained at $\Omega = 0.0$. Like the full curve b with $J_3/J_1 = -0.5$ in figure 2(b), T_{comp} may change in the limited range of Ω. Corresponding to the chain curve in figure 2(a), the chain curve in figure 2(b) also represents the critical boundary line for the existence of T_{comp} in the $T - \Omega$ space. Thus, the results (full curves) in figure 2(b) indicate that the T_{comp} of the bilayer system can be controlled by applying the magnetic field parallel to the bilayer plane (or to the x direction).

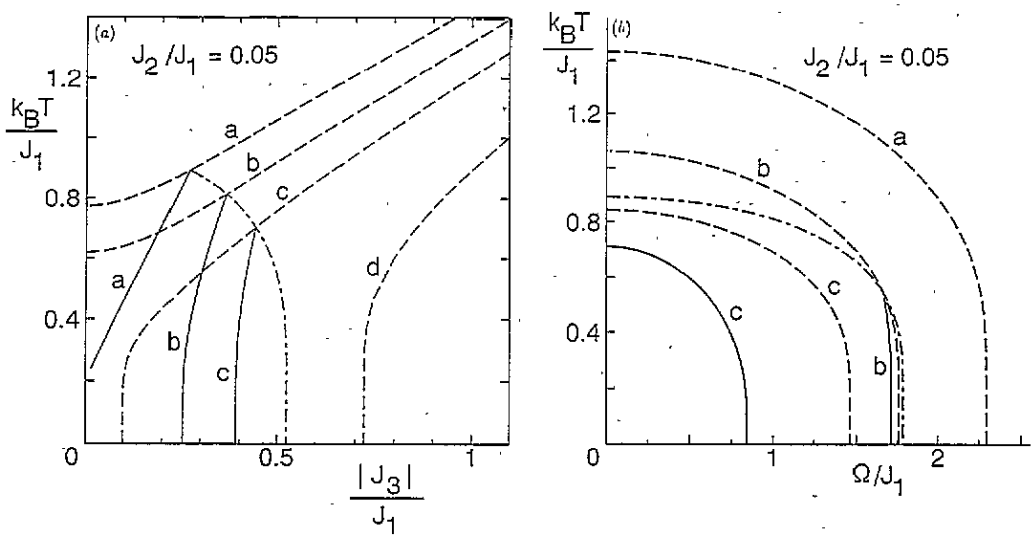

Figure 2. (*a*) Phase diagram (T_{comp} and T_c versus $|J_3|/J_1$) of the bilayer system, when the value of J_2/J_1 is fixed at $J_2/J_1 = 0.05$ and the value of the transverse field Ω is changed: $\Omega/J_1 = 0.0$ (curve a), $\Omega/J_1 = 1.0$ (curve b), $\Omega/J_1 = 1.4$ (curve c) and $\Omega/J_1 = 2.0$ (curve d). The full curves represent the compensation temperatures T_{comp}; the broken curves are the critical temperatures T_c and the chain curve represents a critical boundary line for the existence of the compensation temperature. (*b*) Phase diagram (T_{comp} and T_c versus Ω/J_1) of the bilayer system, when the value of J_2/J_1 is fixed at $J_2/J_1 = 0.05$ and the value of the interlayer coupling J_3/J_1 is changed: $J_3/J_1 = -1.0$ (curve a), $J_3/J_1 = -0.5$ (curve b) and $J_3/J_1 = -0.2$ (curve c). The meaning of the full, broken and chain curves is the same as in (*a*).

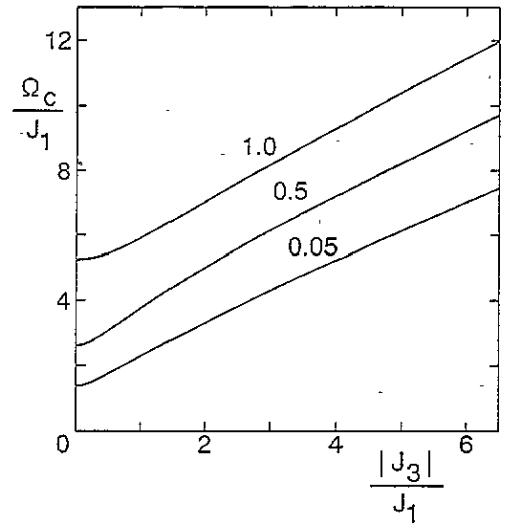

Figure 3. The critical transverse field Ω_c/J_1 as a function of the interlayer coupling $|J_3|J_1$. The numbers accompanying each curve are the values of J_2/J_1.

3.2. Magnetization curve

In this part, let us show some typical temperature dependences of the magnetizations

$(\sigma_z, \sigma_x, m_z, m_x, M_z, M_x)$ in the bilayer system by solving equations (2)–(6) numerically for selected values of J_2, J_3 and Ω in figure 2.

The temperature dependences of σ_α and m_α $(\alpha = x, z)$ for the bilayer system with $J_2/J_1 = 0.05$ and $J_3/J_1 = -0.2$ are depicted in figure 4 by taking different values of Ω/J_1, namely $\Omega/J_1 = 0.1$, 0.5, 1.0 and 2.0. In figure 5, the thermal variations of $|M_z|$ and M_x for the system are also depicted. As is seen from figure 5, the compensation point cannot be obtained in the $|M_z|$ curve labelled $\Omega/J_1 = 1.0$, which is consistent with the result (the full curve c) in figure 2(*b*). Furthermore, when $\Omega/J_1 = 2.0$, the magnetization M_z is always $M_z = 0.0$ in the whole temperature region, while M_x (the broken curve) in figure 5 may decrease from the saturation value at $T = 0$ K. This is also consistent with the result (the broken curve c) in figure 2(*b*).

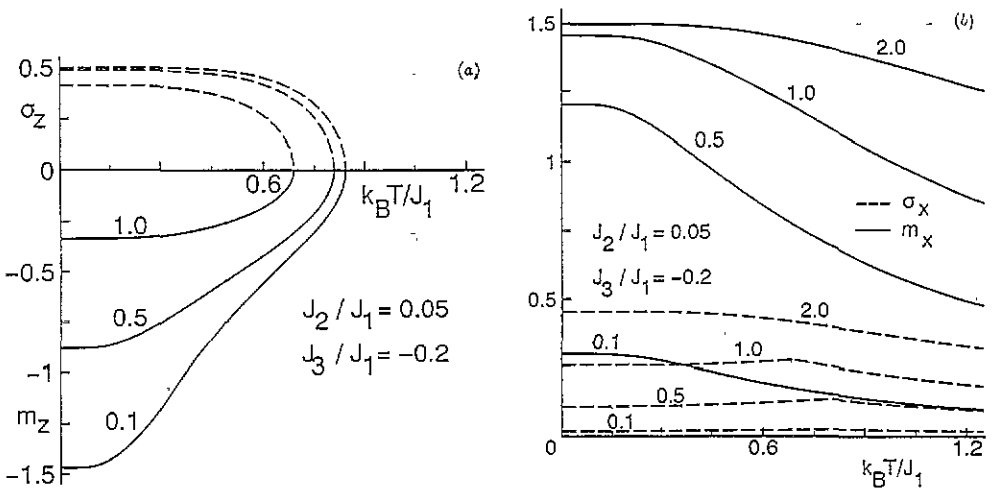

Figure 4. (*a*) The temperature dependences of the longitudinal magnetizations of layer A (broken curves) and layer B (full curves) for the system with $J_2/J_1 = 0.05$ and $J_3/J_1 = -0.2$. The numbers accompanying the curves are the values of Ω/J_1. (*b*) The temperature dependences of the transverse magnetizations of layer A (broken curves) and layer B (full curves) for the system with $J_2/J_1 = 0.05$ and $J_3/J_1 = -0.2$. The numbers accompanying the curves are the values of Ω/J_1.

3.3. Field dependence

In figures 6 and 7, typical transverse-field dependences of the magnetizations for the system with $J_2/J_1 = 0.05$ are given by fixing the temperature at $T = 0.001 J_1/k_B$ and taking three values of J_3/J_1 ($J_3/J_1 = -0.2, -0.5, -1.0$). The Ω dependences of σ_z and m_z are plotted in figure 6(*a*) and the Ω dependences of σ_x and m_x are depicted in figure 6(*b*). Here, notice that the curvatures of σ_x and m_x may change at the value of Ω where σ_z and m_z reduce to zero. In figure 7, the Ω dependences of $|M_\alpha|$ $(\alpha = x, z)$ are given.

4. Specific heat

In this section, let us examine the specific heat of the bilayer system. The internal energy U of the system can be expressed as

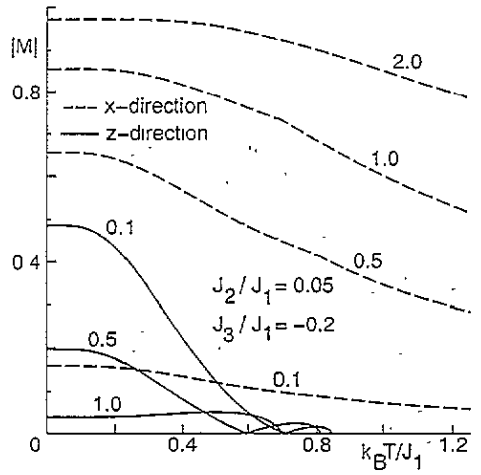

Figure 5. The temperature dependences of the total longitudinal magnetization $|M_z|$ (full curves) and total transverse magnetization M_x (broken curves) for the same system as in figure 4(*b*).

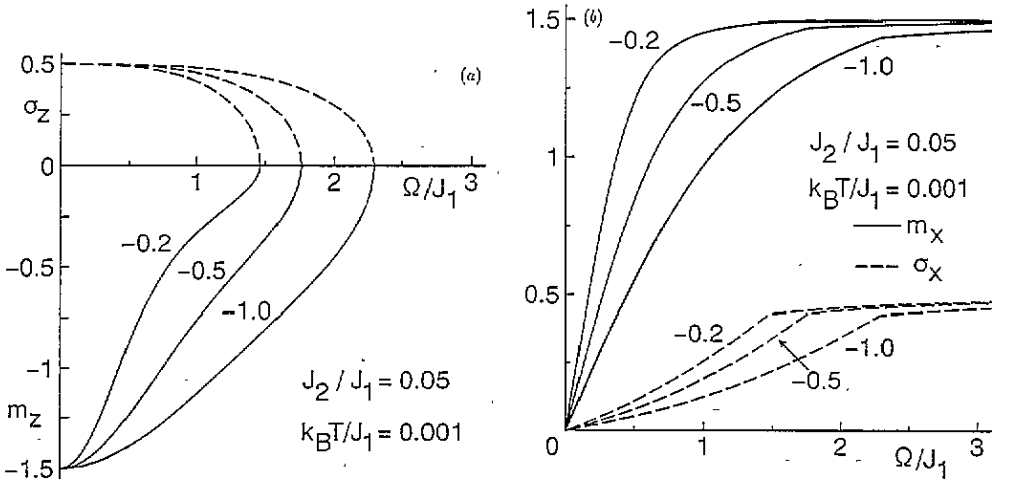

Figure 6. (*a*) The longitudinal magnetization versus transverse field Ω/J_1 for layer A (broken curves) and layer B (full curves), when $J_2/J_1 = 0.05$ and $T = 0.001J_1/k_B$. The numbers accompanying the curves are the values of J_3/J_1. (*b*) The same as in (*a*) but for the transverse magnetizations.

$$U/N = -\tfrac{1}{2}U_A - \tfrac{1}{2}U_B - \Omega(\langle\mu_i^x\rangle + \langle S_m^x\rangle) \tag{12}$$

where U_A and U_B are given by

$$U_A = (\partial/\partial y)\{[\cosh(\tfrac{1}{2}J_1 y) + 2\sigma_z \sinh(\tfrac{1}{2}J_1 y)]^4 \times [\cosh(\eta J_3 y) + (m_z/\eta)\sinh(\eta J_3 y)]^2\}_{y=\nabla} F_A(x)|_{x=0} \tag{13}$$

$$U_B = (\partial/\partial y)\{[\cosh(\eta J_2 y) + (m_z/\eta)\sinh(\eta J_2 y)]^4 \times [\cosh(\tfrac{1}{2}J_3 y) + 2\sigma_z \sinh(\tfrac{1}{2}J_3 y)]^2\}_{y=\nabla} F_B(x)|_{x=0}. \tag{14}$$

Then, the specific heat C can be obtained from the relation

$$C = \partial U/\partial T. \tag{15}$$

Now, in order to evaluate the internal energy (12), it is necessary to know the temperature dependences of σ_z, m_z and η. Their thermal variations have been examined numerically in section 3. In figures 8 and 9, we show some typical behaviours of C (full curves) and U (broken curves) in the bilayer system. Figure 8 shows the temperature dependences of C and U in the bilayer system, fixing the values of J_2 and Ω (or $J_2/J_1 = 0.05$ and $\Omega/J_1 = 0.5$) and changing the value of J_3/J_1. In figure 9, the thermal variations are depicted by selecting the system with $J_2/J_1 = 0.05$ and $J_3/J_1 = -0.2$ in figure 8 and changing the value of Ω.

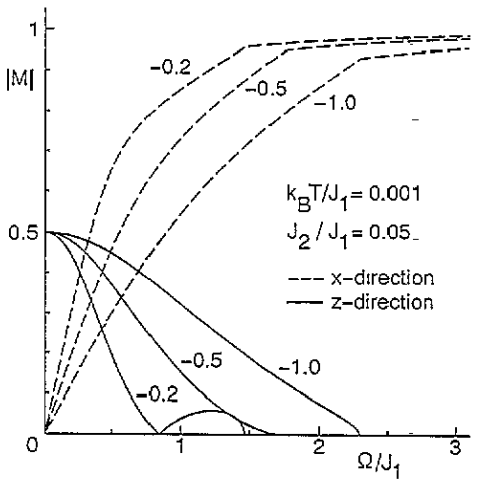

Figure 7. The temperature dependences of the total longitudinal magnetization $|M_z|$ (full curves) and total transverse magnetization M_x (broken curves) for the same system as in figure 6(*a*).

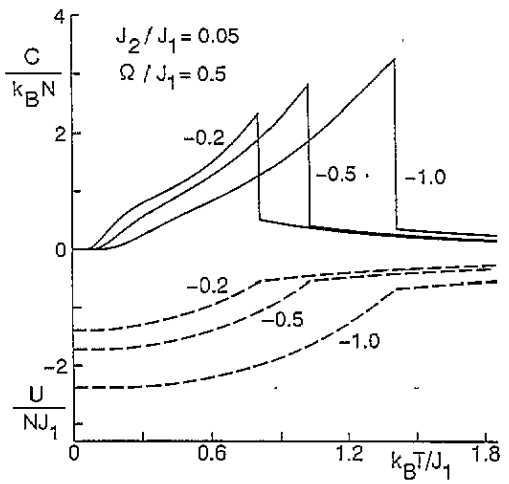

Figure 8. The temperature variations of the specific heat C (full curves) and the internal energy U (broken curves), when $J_2/J_1 = 0.05$ and $\Omega/J_1 = 0.5$. The numbers accompanying each curve are the values of J_3/J_1.

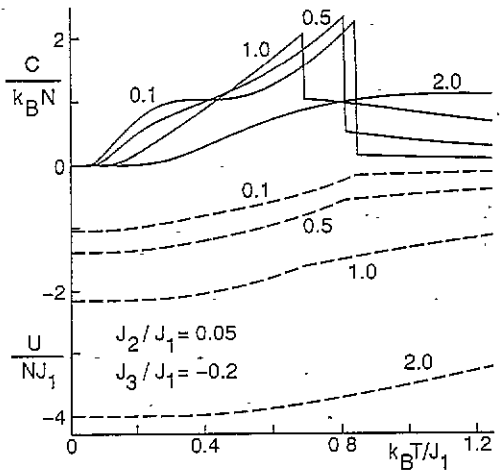

Figure 9. The temperature variations of the specific heat C (full curves) and the internal energy U (broken curves), when $J_2/J_1 = 0.05$ and $J_3/J_1 = -0.2$. The numbers accompanying each curve are the values of Ω/J_1.

As is seen from the figures, the internal energy (broken curves) may express a discontinuity of the curvature at the transition temperature T_c. The discontinuity of C (full curves) at $T = T_c$ in figure 8 becomes larger when the value of $|J_3|/J_1$ increases. In figure 9, on the other hand, the discontinuous gap of C decreases when the value of Ω increases and for $\Omega > \Omega_c$ (or the system with $\Omega/J_1 = 2.0$) there is no discontinuity of C because $T_c = 0.0$ in the system. In particular, figure 9 clearly shows that the specific heat of the system with $J_2/J_1 = 0.05$ and $J_3/J_1 = -0.2$ may show a broad maximum below T_c when the value of Ω is very small. Furthermore, the specific heat in each figure has a finite value even in the region $T > T_c$. This indicates that our formulation includes some spin–spin correlations automatically and is superior to the standard mean-field theory.

5. Conclusions

In this work, we have studied the magnetic properties of the bilayer system with a negative interlayer coupling J_3 in an applied transverse field Ω within the framework of the EFT [12–15]. The bilayer system with an applied transverse field which consists of spin-$\frac{1}{2}$ and spin-$\frac{3}{2}$ ferromagnetic Ising monolayers may show a compensation point in the M_z curve, depending on the strength of J_3 ($J_3 < 0$). By changing the strength of the applied transverse field, the position of the compensation point in the M_z curve can be controlled. In particular, such an investigation may be very important from the technological point of view as well as for academic research, since ferrimagnetic multilayered systems are considered to be possibly useful materials for magneto-optical recording.

As shown in figures 2–9, the magnetic properties of the bilayer system may exhibit characteristic behaviours, depending on the strength of the applied transverse field. As far as we know, little work has been reported on the effects of the applied transverse field on the magnetic properties of these systems. In particular, some of the present results may be related to experimental work on RE/TM multilayer films, since the interlayer coupling J_3 (or 3d–4f indirect interaction) is considered to be negative for heavy REs. In fact, they may show a compensation point for small thicknesses of these materials [3, 5]. However, one must notice some important facts in order to compare the present results with experimental

data for these materials. In this work, we have not included the crystal-field constant in B layers or the existence of disordered interfaces [16]. These are considered to be important for discussing the magnetic properties of real RE/TM multilayer films [17]. These effects will be considered in future work.

Appendix

The functions of F_α, G_α and H_α ($\alpha = \mathrm{A}, \mathrm{B}$) are defined as follows:

$$F_{\mathrm{A}}(x) = (x/2y)\tanh(\tfrac{1}{2}\beta y) \tag{A1}$$

$$H_{\mathrm{A}}(x) = (\Omega/2y)\tanh(\tfrac{1}{2}\beta y) \tag{A2}$$

$$F_{\mathrm{B}}(x) = (x/2y)[3\sinh(\tfrac{3}{2}\beta y) + \sinh(\tfrac{1}{2}\beta y)]/[\cosh(\tfrac{3}{2}\beta y) + \cosh(\tfrac{1}{2}\beta y)] \tag{A3}$$

$$G_{\mathrm{B}}(x) = [3(y^2 + 2x^2)\cosh(\tfrac{3}{2}\beta y) + (y^2 + 6\Omega^2)\cosh(\tfrac{1}{2}\beta y)]/[4\cosh(\tfrac{3}{2}\beta y) + 4\cosh(\tfrac{1}{2}\beta y)]y^2 \tag{A4}$$

$$H_{\mathrm{B}}(x) = (\Omega/2y)[3\sinh(\tfrac{3}{2}\beta y) + \sinh(\tfrac{1}{2}\beta y)]/[\cosh(\tfrac{3}{2}\beta y) + \cosh(\tfrac{1}{2}\beta y)] \tag{A5}$$

where $\beta = (k_{\mathrm{B}}T)^{-1}$ and $y = \sqrt{\Omega^2 + x^2}$.

References

[1] Kamiguchi Y, Hayakawa Y and Fujimori H 1989 *Appl. Phys. Lett.* **55** 1918
[2] Tejada T, Badia F, Martinez B and Ruiz J M 1991 *J. Magn. Magn. Mater.* **101** 181
[3] Ertl L, Endl G and Hoffmann H 1982 *J. Magn. Magn. Mater.* **113** 227
[4] Sajieddine M, Bauer Ph, Dufour C, Cherifi K, Marchal G and Mangin Ph 1992 *J. Magn. Magn. Mater.* **113** 243
[5] Endl G, Bielmeier B and Hoffmann H 1991 *Coll. Digest 13th Int. Coll. on Magnetic Films and Surfaces (Glagow. 1991)* p 155
[6] Hinckey L L and Mills D L 1985 *J. Appl. Phys.* **57** 3687
[7] Kaneyoshi T and Beyer H 1980 *J. Phys. Soc. Japan* **49** 1306
[8] Albuquerque E I, Sarmento E F and Tilley D F 1986 *Solid State Commun.* **58** 41
[9] Ferrenberg A M and Landau D P 1991 *J. Appl. Phys.* **70** 6125
[10] Hai T, Li Z Y, Lin D L and George T F 1991 *J. Magn. Magn. Mater.* **79** 227
[11] Cottam M G and Tilley D R 1989 *Introduction to Surface and Superlattice Excitation* (Cambridge: Cambridge University Press)
[12] Kaneyoshi T and Jaščur M 1993 *J. Magn. Magn. Mater.* **118** 17
[13] Kaneyoshi T, Tucker J W and Jaščur M 1992 *Physica* A **186** 495
[14] Kaneyoshi T, Jaščur M and Fittipaldi I P 1993 *Phys. Rev.* B **48** at press
[15] Kaneyoshi T 1993 *Acta Phys. Polonica* A at press
[16] Khater A, Le Gal G and Kaneyoshi T 1992 *Phys. Lett.* **171A** 237
Benyoussef A and Kaneyoshi T 1993 *Phys. Lett.* **173A** 411
[17] Kaneyoshi T 1991 *J. Phys.: Condens. Matter* **3** 4497